Anal. Chem. **2007,** *79,* 4056−4065

Naked-Eye Cadmium Sensor: Using Chromoionophore Arrays of Langmuir−Blodgett Molecular Assemblies

Deivasigamani Prabhakaran, Ma Yuehong, Hiroshi Nanjo, and Hideyuki Matsunaga*

Research Center for Compact Chemical Process, National Institute of Advanced Industrial Science and Technology (AIST Tohoku), Sendai 983-8551, Japan

This study demonstrates the possibility of a reversible naked-eye detection method for submicromolar levels of cadmium(II) using the Langmuir−Blodgett (L-B) technique. Molecular assemblies of 4-*n*-dodecyl-6-(2-thiazolylazo)resorcinol are transferred on precleaned microscopic glass slides, to act as a sensing probe. Isotherm ($\pi-A$) measurements were performed to ensure the films' structural rigidity and homogeneity during sensor fabrication. The sensor surface morphology was characterized using atomic force microscopy and scanning electron microscopy. The probe membrane exhibits visual color transition, forming a series of reddish-orange to pinkish-purple complexes with cadmium, over a wide concentration range (0.04−44.5 μM). Cadmium response kinetics and the changes in the sensors' intrinsic optical properties were monitored using absorption spectroscopy and further confirmed using X-ray photoelectron spectroscopy. A hybrid L-B film composite of poly(vinyl stearate) and poly(vinyl-*N*-octadecylcarbamate) were investigated for enhancing sensor performance. The sensor was tested for its practical approach to prove its cadmium selectivity and sensitivity amid common matrix constituents using synthetic mixtures and real water samples. Using the sensor strips, the respective lower limits of cadmium detection and quantification are 0.039 and 0.050 μM, as estimated from a normalized linear calibration plot.

Design of a metal ion sensor has been sought through many research efforts related to applications such as clinical toxicology, environmental bioinorganic chemistry, bioremediation, and waste management.[1−3] Cadmium is a nonessential element that is toxic for humans because it forms a strong bond with sulfur and can therefore displace essential metal ions such as Zn^{2+} and Ca^{2+} from the binding sites of certain enzymes.[4−6] Cadmium finds major applications in the production of nickel−cadmium rechargeable batteries, smelting, phosphate fertilizers, ceramic enamels, and paint pigments, thereby rendering it a species that is certain to be dispersed into the environment.[7,8] It is also estimated that cadmium ions are released into the atmosphere through natural phenomena such as erosion, abrasion, and volcanic eruption. Consequently, cadmium is naturally found in water, soil, and food, with its average content placed generally between 0.1 and 0.5 ppm in the earth's crust.[9] Numerous quantitative testing methods are available for cadmium(II), but because of the high setup and running costs of sophisticated instrumental methods such as atomic absorption spectrometry (AAS),[10] inductively coupled plasma atomic emission spectrometry (ICP-AES),[11] inductively coupled plasma mass spectrometry,[12] and electrochemical devices,[13] small local governments and developing countries cannot realistically make practical use of them. Although good analytical

* To whom correspondence should be addressed. Tel.: (+81) 22-237-3072. Fax: (+81) 22-237-7027. E-mail: hide.matsunaga@aist.go.jp.

(1) (a) Walkup, G.K.; Imperiali, B. *J. Am. Chem. Soc.* **1996**, *118*, 3053−3054. (b) Liu, J.; Lu, Y. *J. Am. Chem. Soc.* **2004**, *126*, 12298−12305.

(2) (a) Deo, S.; Godwin, H. A. *J. Am. Chem. Soc.* **2000**, *122*, 174−175. (b) Li, J.; Lu, Y. *J. Am. Chem. Soc.* **2000**, *122*, 10466−10467.

(3) (a) Miyawaki, A.; Llopis, J.; Helm, R.; McCaffery, J. M.; Adams, J. A.; Ikura, M.; Tsien, R. Y. *Nature* **1997**, *388*, 882−887. (b) Chen, P.; He, C. *J. Am. Chem. Soc.* **2004**, *126*, 728−729.

(4) (a) Goel, J.; Kadirvelu, K.; Rajagopal, C.; Garg, V. K. *Ind. Eng. Chem. Res.* **2006**, *45*, 6531−6537. (b) Wang, C.; Fang, Y.; Peng, S.; Ma, D.; Zhao, J. *Chem. Res. Toxicol.* **1999**, *12*, 331−334.

(5) (a) Lofts, S.; Spurgeon, D.; Svendsen, C. *Environ. Sci. Technol.* **2005**, *39*, 8533−8540. (b) Martelli, A.; Rousselet, E.; Dycke, C.; Bouron, A.; Moulis, J.-M. *Biochimie* **2006**, *88*, 1707−1719.

(6) (a) Arvidson, B. *Toxicology* **1994**, *88*, 1−14. (b) Prozialeck, W. C.; Edwards, J. R.; Woods, J. M. *Life Sci.* **2006**, *79*, 1493−1506. (c) Cerullia, N.; Campanellab, L.; Grossib, R.; Politic, L.; Scandurrac, R.; Giovanni, S.; Galloe, F.; Damianie, S.; Alimontif, A.; Petruccif, F.; Carolif, S. J. *Trace Elem. Med. Biol.* **2006**, *20*, 171−179.

(7) (a) Clement, R. E.; Yang, P. W.; Koester, C. J. *Anal. Chem.* **1999**, *71*, 257−292. (b) Thaller, L. H.; Zimmerman, A. H. *J. Power Sources* **1996**, *63*, 53−61.

(8) (a) Hamon, R. E.; McLaughlin, M. J.; Naidu, R.; Correll, R. *Environ. Sci. Technol.* **1998**, *32*, 3699−3703. (b) Bailey, S. E.; Olin, T. J.; Bricka, R. M.; Adrian, D. D. *Water Res.* **1999**, *33*, 2469−2479.

(9) Kirk, R. E.; Othmer, D. F. *Encyclopedia of Chemical Technology*; Interscience Inc.: New York, 1982.

(10) (a) Wang, Y.; Wang, Y.-H.; Fang, Z.-L. *Anal. Chem.* **2005**, *77*, 5396−5401. (b) Ye, Q.-Y.; Li, Y.; Jiang, Y.; Yan, X.-P. *J. Agric. Food Chem.* **2003**, *51*, 2111−2114.

(11) (a) Bings, N. H.; Bogaerts, A.; Broekaert, J. A. C. *Anal. Chem.* **2002**, *74*, 2671−2712. (b) Pyle, S. M.; Nocerino, J. M.; Deming, S. N.; Palasota, J. A.; Palasota, J. M.; Miller, E. L.; Hillman, D. C.; Kuharic, C. A.; Cole, W. H.; Fitzpatrick, P. M.; Watson, M. A.; Nichols, K. D. *Environ. Sci. Technol.* **1996**, *30*, 204−213.

(12) (a) Cloquet, C.; Corrigan, J.; Libourel, G.; Sterckeman, T.; Perdrix, E. *Environ. Sci. Technol.* **2006**, *40*, 2525−2530. (b) Dolan, S. P.; Nortrup, D. A.; Bolger, P. M.; Capar, S. G. *J. Agric. Food Chem.* **2003**, *51*, 1307−1312.

(13) (a) Pongratz, R.; Heumann, K.G. *Anal. Chem.* **1996**, *68*, 1262−1266. (b) Shtoyko, T.; Conklin, S.; Maghasi, A. T.; Piruska, A.; Richardson, J. N.; Seliskar, C. J.; Heineman, W. R. *Anal. Chem.* **2004**, *76*, 1466−1473. (c) Honeychurch, K. C.; Hart, J. P. *Trends Anal. Chem.* **2003**, *22*, 456−469. (d) Bakker, E.; Pretsch, E. *Trends Anal. Chem.* **2005**, *24*, 199−207.

10.1021/ac0623540 CCC: $37.00
Published on Web 04/21/2007

performance is obtainable with pretreatment techniques such as solvent extraction[14,15] and solid-phase extraction,[16,17] they are normally associated with complicated treatment procedures, large volumes of reagent/solvent consumption, and unsatisfactory enrichment factors.[18] For those reasons, development of smart, simple, and compact analytical methods for toxicity validation has been an area of prime research concern. In recent years, sensor technology is considered as one of the few potential candidates for environmental monitoring.[19] Considerable attention has been devoted to the design of supramolecules and chromoionophores that can recognize target analytes selectively through visual detection and optical responses.[20−23] However, developing such sensing materials has not been an easy task because of many factors, which include tedious synthesis, supporting electronic devices, insufficient ion selectivity, and sensitivity. Analytical researchers are intent upon developing new minimized and green methods using nanotechnology and nanoscale materials, which constitute a new and exciting field of research to overcome these looming problems.

Langmuir−Blodgett (L-B) thin-film technique has been a key manufacturing tool in nanotechnology, with applications ranging from biotechnology (membranes and biosensors), gas sensors, and electronic devices to lithography.[24−26] Interest in L-B technique is fueled by its merits, which include (a) precise control of the monolayer thickness, (b) homogeneous deposition of the monolayers over large areas, and (c) the possibility of generating multilayer structures with varying layer composition on almost any kind of solid substrate.[27,28] It has been observed that L-B monolayers of metal complexes have properties similar to those of supramolecular structures involved in the biosensing of Li^+, Na^+, K^+, Ca^{2+}, etc.[29,30] Therefore, incorporation of L-B molecular layers of chelating groups onto solid platforms is expected to reveal meaningful applications in sensing techniques and other fundamental studies. However, such implications of L-B film monolayers in toxicity validation have remained only vague conjecture, especially in the emerging areas of naked-eye sensing. In that context, we intend to fabricate a smart visual ion sensor based on L-B methodology that can fulfill major analytical needs in environmental monitoring.

In this study, we report for the first time the use of chemically synthesized amphiphilic 4-*n*-dodecyl-6-(2-thiazolylazo)resorcinol (DTAR) monolayers as a potential solid-state chromoionophore sensor for detecting trace levels of cadmium(II). The sensor kit provides two means of cadmium detection: one by mere naked-eye detection of the visual color transition, and the other by precise measurement of the relative changes of the sensor optical properties. The sensor strips were selective and sensitive for cadmium ions without major interference from coexisting transition ions and other cationic and anionic species. The sensor strips were reversible and reusable without marked loss in their sensing efficiency up to four repeated cycles. It was inferred that the combined use of polymer composite with the chromoionophore molecular assemblies provided a better way to produce mechanically stable optical sensors. The fabricated LB film sensor was found to be both promising and reliable for rapid and selective detection of submicromolar cadmium ions from highly saline samples. To our knowledge, this sensor marks the first step in developing a naked-eye cadmium sensor using L-B nanoassemblies.

EXPERIMENTAL SECTION

Instrumentation. An L-B film developing instrument (NL-LB-200 Film Deposition System; Nippon Laser and Electronics Lab.)

(14) (a) Huynh, H. T.; Tanaka, M. *Ind. Eng. Chem. Res.* **2003**, *42*, 4050−4054. (b) SenGupta, A. K.; Marcus, Y. *Ion Exchange and Solvent Extraction*; Marcel Dekker, Inc.: New York, 2004. (c) Vanderpool, R. A.; Buckley, W. T. *Anal. Chem.* **1999**, *71*, 652−659.

(15) (a) Almela, A.; Elizalde, M. P. *Hydrometallurgy* **1995**, *37*, 47−57. (b) Nogueira, C. A.; Delmas, F. *Hydrometallurgy* **1999**, *52*, 267−287. (c) Yoshinaga, J.; Morita, M.; Edmonds, J. S. *J. Anal. At. Spectrom.* **1999**, *14*, 1589−1592.

(16) (a) Rao, T. P.; Kala, R.; Daniel, S. *Anal. Chim. Acta* **2006**, *578*, 105−116. (b) Rao, T. P.; Daniel, S.; Gladis, J. M. *Trends Anal. Chem.* **2004**, *23*, 28−35. (c) Sarzanini, C.; Bruzzoniti, M. C. *Trends Anal. Chem.* **2001**, *20*, 304−310.

(17) (a) Fritz, J. S. *Analytical Solid-Phase Extraction*; Wiley-VCH: New York, 1999. (b) Altria, K. D. *J. Chromatogr., A* **1999**, *1−2*, 443−463. (c) Lin, Y.; Smart, N. G.; Wai, C. M. *Trends Anal. Chem.* **1995**, *14*, 123−133.

(18) (a) Cave, M. R.; Butler, O.; Cook, J. M.; Cresser, M. S.; Miles, D. L. *J. Anal. At. Spectrom.* **2000**, *15*, 181. (b) Shi, J.; Zhu, Y.; Zhang, X.; Baeyens, W. R. G.; Garcia-Campana, A. M. *Trends Anal. Chem.* **2004**, *23*, 351−360. (c) Simpson, N. J. K. *Solid Phase Extraction, Principle, Techniques and Applications*; Marcel Dekker, Inc.: New York, 2000.

(19) Niessner, R. *Trends Anal. Chem.* **1991**, *10*, 310−316.

(20) (a) Gunnlaugsson, T.; Lee, T. C.; Parkesh, R. *Org. Lett.* **2003**, *5*, 4065−4068. (b) Bronson, R. T.; Michaelis, D. J.; Lamb, R. D.; Husseini, G. A.; Farnsworth, P. B.; Linford, M. R.; Izatt, R. M.; Bradshaw, J. S.; Savage, P. B. *Org. Lett.* **2005**, *7*, 1105−1108.

(21) (a) Wolfbeis, O. S. *Mikrochim. Acta* **1997**, *126*, 117−192. (b) Resendiz, M. J. E.; Noveron, J. C.; Disteldorf, H.; Fischer, S.; Stang, P. J. *Org. Lett.* **2004**, *6*, 651−653. (c) Balaji, T.; Sasidharan, M.; Matsunaga, H. *Anal. Bioanal. Chem.* **2006**, *384*, 488−494.

(22) (a) Mayr, T.; Igel, C.; Liebsch, G.; Klimant, I.; Wolfbeis, O. S. *Anal. Chem.* **2003**, *75*, 4389−4396. (b) Preininger, C.; Wolfbeis, O. S. *Biosens. Bioelectron.* **1996**, *11*, 981−990. (c) Czolk, R.; Reichert, J.; Ache, H. J. *Sens. Actuators, A: Phys.* **1991**, *26*, 439−41.

(23) (a) Chapman, P. M.; Riddle, M. J. *Environ. Sci. Technol.* **2005**, *39*, 200A−206A. (b) Aragoni, M. C.; Arca, M.; Demartin, F.; Devillanova, F. A.; Isaia, F.; Garau, A.; Lippolis, V.; Jalali, F.; Papke, U.; Shamsipur, M.; Tei, L.; Yari, A.; Verani, G. *Inorg. Chem.* **2002**, *41*, 6623−6632.

(24) (a) Badr, H. A. I.; Meyerhoff, E.M. *J. Am. Chem. Soc.* **2005**, *127*, 5318−5319. (b) Mayes, A. G.; Blyth, J.; Millington, R. B.; Lowe, C. R. *Anal. Chem.* **2002**, *74*, 3649−3657. (c) Umezawa, Y.; Roki, H. *Anal. Chem.* **2004**, 321A−326A. (d) Liu, M.; Ushida, K.; Kira, A.; Nakahara, H. *J. Phys. Chem. B* **1997**, *101*, 1101.

(25) (a) Henrichs, S.; Collier, C. P.; Saykally, R. J.; Shen, Y. R.; Heath, J. R. *J. Am. Chem. Soc.* **2003**, *122*, 4077−4083. (b) Petty, M. C. *Thin Solid Film* **1992**, *210−211*, 417−426. (c) Hamley, I. W. *Angew. Chem., Int. Ed.* **2003**, *42*, 1692−1712. (d) Fujiki, M.; Tabei, H. *Langmuir* **1988**, *4*, 320−326.

(26) (a) Valli, L. *Adv. Colloid Interface Sci.* **2005**, *116*, 13−44. (b) Barlow, W. A. *Langmuir-Blodgett Films*; Elsevier Publisher: Amsterdam, 1980. Lvov, Y.; Decher, G.; Möhwald, H. *Langmuir* **1993**, *9*, 481−486. (c) Moriizumi, T. *Thin Solid Films* **1998**, *160*, 413−419. (d) Ferreira, M.; Riul, A., Jr.; Wohnrath, K.; Fonseca, F. J.; Oliveira, O. N.; Jr.; Mattoso, L. H. C. *Anal. Chem.* **2003**, *75*, 953−955.

(27) (a) Petty, M. C. *Langmuir Blodgett Technique-An Introduction*; Cambridge University Press: New York, 1996. (b) Decher, G. *Science* **1997**, *277*, 1232−1237. (c) Nagel, J.; Oertel, U.; Friedel, P.; Komber, H.; Mobius, D. *Langmuir* **1997**, *13*, 4693−4698.

(28) (a) Ledner, I. K.; Petty, M. C. *Adv. Mater.* **1996**, *8*, 615−630. (b) Graf, K.; Riegler, H. *Colloid Surf. A: Physicochem. Eng. Aspects* **1998**, *131*, 215−224. (b) Ng, S. C.; Zhou, X. C.; Chen, Z. K.; Miao, P.; Chan, H. S. O.; Li, S. F. Y.; Fu, P. *Langmuir* **1998**, *14*, 1748−1752. (c) Cheek, B. J.; Steel, A. B.; Miller, C. J. *Langmuir* **2000**, *16*, 10334−10339.

(29) (a) Rochefeuille, S.; Jimenez, C.; Tingry, S.; Seta, P.; Desfours, J. P. *Materials Sci. Eng. C* **2002**, *21*, 43−46. (b) Wang, E.; Ding, L.; Li, J.; Dong, S. *Thin Solid Films* **1997**, *293*, 153−158. (c) Wolfbeis, O. S.; Bernhard, P.; Schaffar, H. *Anal. Chim. Acta* **1987**, *198*, 1−12.

(30) (a) Reichert, W. M.; Bruckner, J.; Joseph, J. *Thin Solid Films* **1987**, *152*, 345−376. (b) Palacin, S. *Adv. Colloid Interface Sci.* **2000**, *87*, 165−181. (c) Girard, A. P.-E.; Godoy, S.; Blum, J. L. *Adv. Colloid Interface Sci.* **2005**, *16*, 205−225.

was used for measuring the pressure (π)−area (A) isotherm and the transfer ratio (τ). Structural features of the synthesized probe molecules were characterized using an FT-IR spectrophotometer (IRPrestige-21; Shimadzu Corp.); its purity was ascertained using CHN elemental analysis (JM10 Microcorder; J-Science Lab.). A UV−vis spectrophotometer (UV-3150; Shimadzu Corp.) equipped with a detachable solid sample compartment was used to measure the absorption spectra of the sensor's optical changes. The surface morphology of the probe membrane was studied using tapping-mode atomic force microscopy (AFM; NanoScope IIIa; Digital Instruments) and by scanning electron microscopy (SEM) (Miniscope TM-1000; Hitachi Ltd.) imaging. The confirmation of cadmium chelation with an L-B film probe was studied using XPS (PHI 5601ci; Ulvac) analysis, using Mg Kα X-ray source (14 kV, 400 W). The residual metal ions in the aqueous phase after equilibration were determined using ICP-AES (SPS-1500; Seiko Instruments Inc.) analysis. A water bath incubator built into a mechanical shaker (BT-100; Yamato Co. Ltd.) was used for batch equilibration studies. A portable pH/Ion meter (D-53; Horiba Ltd.) was used for measuring the subphase (water) pH during L-B isotherm and film transfer.

Reagents and Procedures. All reagents, solvents, and chemicals procured for probe synthesis and subsequently for sensor fabrication were of high-purity grade (Wako Pure Chemical Industries Ltd., Osaka, Japan) and were used without further purification. For sensor protection, four amphiphilic polymers (poly(vinyl-*N*-octadecylcarbamate) (PVOC), poly(vinyl stearate) (PVS), poly(maleic anhydride-*alt*-1-octadecene) (PMO), and poly-(octadecyl methacrylate) (POMA)) were studied; they were procured from Aldrich Chemical Co. Inc. (Milwaukee, WI). Individual metal ion stock solutions were prepared from AAS-grade standard solutions (1000 ppm (μg/mL) in 0.01 mol/L HNO_3), purchased from Wako Pure Chemical Industries Ltd. For pH adjustment, Good's buffers (0.2 mol/L, Dojindo Laboratories, Kumamoto, Japan), consisting of 3-morpholinopropanesulfonic acid (MOPS)−NaOH (pH 6−9), 2-(cyclohexylamino)ethanesulfonic acid (CHES)−NaOH (pH 9−10), and *N*-cyclohexyl-3-aminopropanesulfonic acid (CAPS)−NaOH (pH 10−12), were used. Precleaned microslide glass plates (0.8−1.0 mm thick and 38 × 13 mm, S-111 type; Matsunami Glass Ind. Ltd.) were used as solid substrates for probe-anchoring.

The amphiphilic chromophore (DTAR) was synthesized under freezing conditions using equimolar coupling of prediazotized 2-aminothiazole with 4-dodecylresorcinol. The product was obtained as a dark red precipitate and was purified through repeated recrystallization from hot ethanol.[31] The details of probe synthesis and its characterization are provided in Supporting Information. Based on spectral characteristics of 2-thiazolylazoresorcinol, at pH <6.9, the probe (DTAR) exists as a neutral species (H_2L) with a λ_{max} at 455 nm (ϵ − 1.99 × 10^4 L mol^{-1} cm^{-1}). The visible absorption spectra of DTAR (25 μM) were measured after extraction into 4-methyl-2-pentanone. Solvent extraction studies confirmed that the DTAR molecules can be extracted as a neutral H_2L species, under these conditions. The monoanionic species (HL^-) and dianionic species (L^{2-}) were extracted respectively as ion pairs with sodium ion, with a λ_{max} at 495 and 539 nm. The

(31) Ueno, K.; Imamura, T.; Cheng, K. L. *Handbook of Organic Analytical Reagents*, 2nd ed.; CRC Press: Boca Raton, FL, 1992; pp 205−206.

Chart 1. Structure of Sensing Probe and Its Four Protecting Polymers

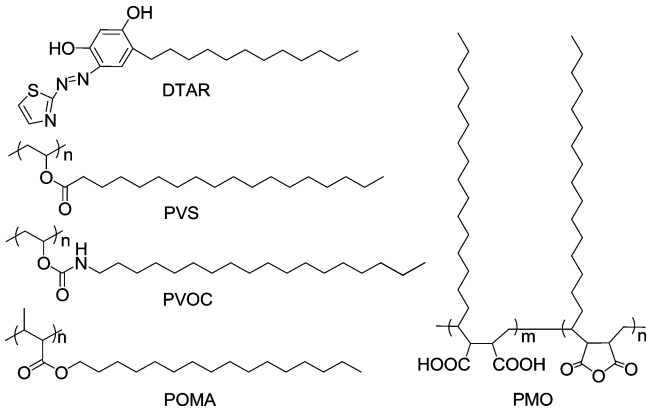

molecular structure of the chromoionophore and the four polymers studied for sensor stability are depicted in Chart 1.

Fabrication of DTAR Multilayer Film Assembly. For sensor fabrication, the probe and the four polymers were dissolved respectively in high-purity grade benzene and chloroform. The pressure (π)−area (A) isotherm plots were measured to elucidate the phase transition of the structural orientation and film stability of the probe and polymer layers. On the basis of their individual limiting collapse pressure (from the isotherm plot), the target pressures were set to achieve a film transfer of greater homogeneity and uniformity. The fabrication of L-B films and the layer-by-layer transfer of molecular assemblies involve the following sequence: (a) microdroplets of probe and polymer solutions were spread evenly on the water subphase of a moving-wall L-B film fabrication system; (b) after solvent evaporation, the surface pressure was increased to its target pressure by film compression, using a Teflon barrier; and (c) upon attaining equilibration, the compressed film layers were eventually transferred as self-organized L-B monolayers at the air−water interface by vertical dipping of the planar glass substrate. During film transfer, the surface pressure was maintained using a computer-controlled feedback system.

Isotherm Plots and Transfer Ratios. The pressure (π)−area (A) isotherm for the DTAR, PVOC, PVS, PMO, and POMA monolayers generated at the air−water interface is shown in Figure 1A. The isotherm plot for DTAR film exhibits a first phase transition at 36.3 Å^2 that should correspond to the nonplanar to planar conformation of the thiazole and phenyl rings, with the dodecyl chain oriented outward from the water surface. With increasing compression, the isotherm observed after 25 mN/m with a molecular area of ~32.9 Å^2 corresponds to the transition from liquid-expanded to a more condensed state, reaching to its limiting pressure at 37.5 mN/m. In the case of polymer films, their isotherm exhibits a two-phase transition of molecular orientation, first from the liquid-expanded gaseous phase to a liquid-expanded phase, with respective mean molecular areas of 27.0, 35.1, 39.2, and 50.7 Å,^{2} for POMA, PMO, PVS, and PVOC. This phase transition possibly explains the gauche conformation acquired using the long alkyl units. The second transition to an ordered, liquid-expanded condensed state was observed at 22.1, 27.9, 33.0, and 43.3 Å^2 for POMA, PMO, PVS, and PVOC, respectively, corresponding to surface pressure of 15.2, 47.1, 51.7, and 45.5 mN/

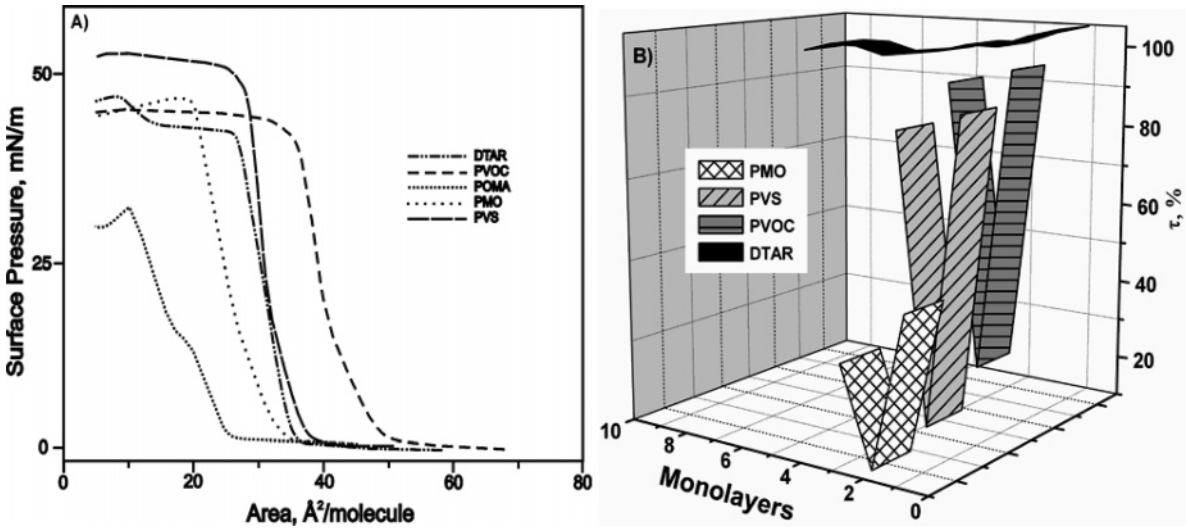

Figure 1. (A) Surface pressure (π) vs area (A) isotherm of DTAR, PVOC, POMA, PMO, and PVS films at the air−water interface at 20 °C obtained by compression at a rate of 10 mm/min. (B) (%) Transfer ratio (τ) values observed for DTAR 10 layers, and for PVOC, PMO, and PVS (3 layers each) on DTAR10.

Table 1. Optimized Instrumental and Experimental Parameters

parameters	DTAR	PVOC	PVS	mixed ratio
limiting pressure (mN/m)	38	45	51.5	37
target pressure (mN/m)	28	40	43	32
barrier speed (mm/min)	10	10	10	10
dipper upstroke (mm/min)	0.25	0.10	0.10	0.15
dipper downstroke (mm/min)	0.25	-	0.10	0.10
concentration (mM)	1	1	1	1
volume (μL) range	85−100	75−80	75−85	120−150
dipper up stay time (s)	600	600	600	600
dipper down stay time (s)	60	60	60	60

m, prior to film collapse. The isotherm plot for POMA indicates that the polymer does not form stable layers on the water subphase; hence, PVOC, PVS and PMO films were investigated to ensure sufficient cohesion of the polymer monolayers on the transferred probe monolayers.

The mechanism of monolayer transfer onto hydrophilic SiO_2 (glass) substrate was investigated, where the probe monolayers exhibits a homogeneous Y-type film deposition pattern. The extent of deposition was measured in terms of transfer ratio (τ), defined as the ratio of monolayer area occupied on the water surface (A_L) and the solid substrate (A_S): $\tau = A_L/A_S$.[32] For a homogeneous film coating, a τ value of 1 ± 0.05 was achieved during each (DTAR) monolayer transfer (Figure 1B). However, with polymer films, τ values of ≤ 0.97 and ≥ 0.25 for PVOC and ≤ 0.89 and ≥ 0.15 for PVS were achieved, respectively, for the upstroke and downstroke (Figure 1B). This helps in predicting that both polymers exhibit a mixed Z-type (head-to-tail) pattern, with a prominent monolayer transfer during the upstroke. However, for PMO, a τ value of ≤ 0.5 and ≥ 0.15 was observed for upstrokes and downstrokes, despite greater film rigidity. For the efficient protection of the probe molecular assemblies, the polymer monolayers are expected to have higher τ values to ensure greater surface coverage. Based on preliminary studies, it was predicted that PMO monolayers are unsuitable for sensor protection. Table 1 shows optimized instrumental parameters for generating an efficient sensing system; precedent studies of the mixing ratios of hybrid probe−polymer composite will be described in subsequent sections.

Analytical Method for Ion Sensing. Aqueous-phase equilibration of sensor strips with cadmium ions was performed using a batch equilibration method. For ion sensing, sensor strips were equilibrated for specific time durations at 200 rpm in 50-mL-capacity containers holding 30 mL of overall sample volume, including 3−4 mL of MOPS buffer (pH 7.5). Optimization of sensor working parameters was normally performed at 30−40 °C, unless otherwise specified. Buffer solutions were adjusted to ambient pH using a microcomputerized pH/Ion meter (F-24 model; Horiba Ltd.). After phase equilibration, the residual aqueous-phase metal ion concentrations were estimated using ICP-AES. Metal ion concentrations are expressed either in terms of parts per million (ppm, mg/L or μg/mL), in parts per billion (ppb, μg/L), or in molarity (M, mol/L). For sensor regeneration, a 20-mL volume of 0.1 M HCl or EDTA was used as a cadmium decomplexing agent.

RESULTS AND DISCUSSION

Characterization of Film Sensor Surface Morphology. XPS analyses of the DTAR 10-layered film sensor assembly confirms the elemental presence of N=N and OH groups along with the thiazole unit. The analysis was performed in a sample chamber pressure maintained under 10^{-7} MPa and the binding energy scales were adjusted to the highest $C_{(1s)}$ peak position equal to 285 eV. Figure 2A depicts the XPS plot for a Cd^{2+} chelate probe assembly, with a characteristic $Cd_{(3d)}$ peak corresponding to the binding energy of 405 eV. The surface topographic image of a cadmium-complexed, five-layered DTAR assembly, observed using tapping-mode AFM (Figure 2B), reflects a distorted peak−valley domain structure with few holes, associated with the distorted molecular orientation of probe monolayers, attributable to the steric influence of cadmium inclusion. In addition, AFM imaging of 10-layer probe strips at different cadmium(II) concentrations (1.25, 0.75, and 0.25 μM) clearly illustrates the diminishing size of the membrane cavity with increasing cadmium chelation (right

(32) Ullman, A. *An Introduction to Ultra Thin Organic Films from Langmuir-Blodgett to Self-Assembly*; Academic Press Inc.: New York, 1991.

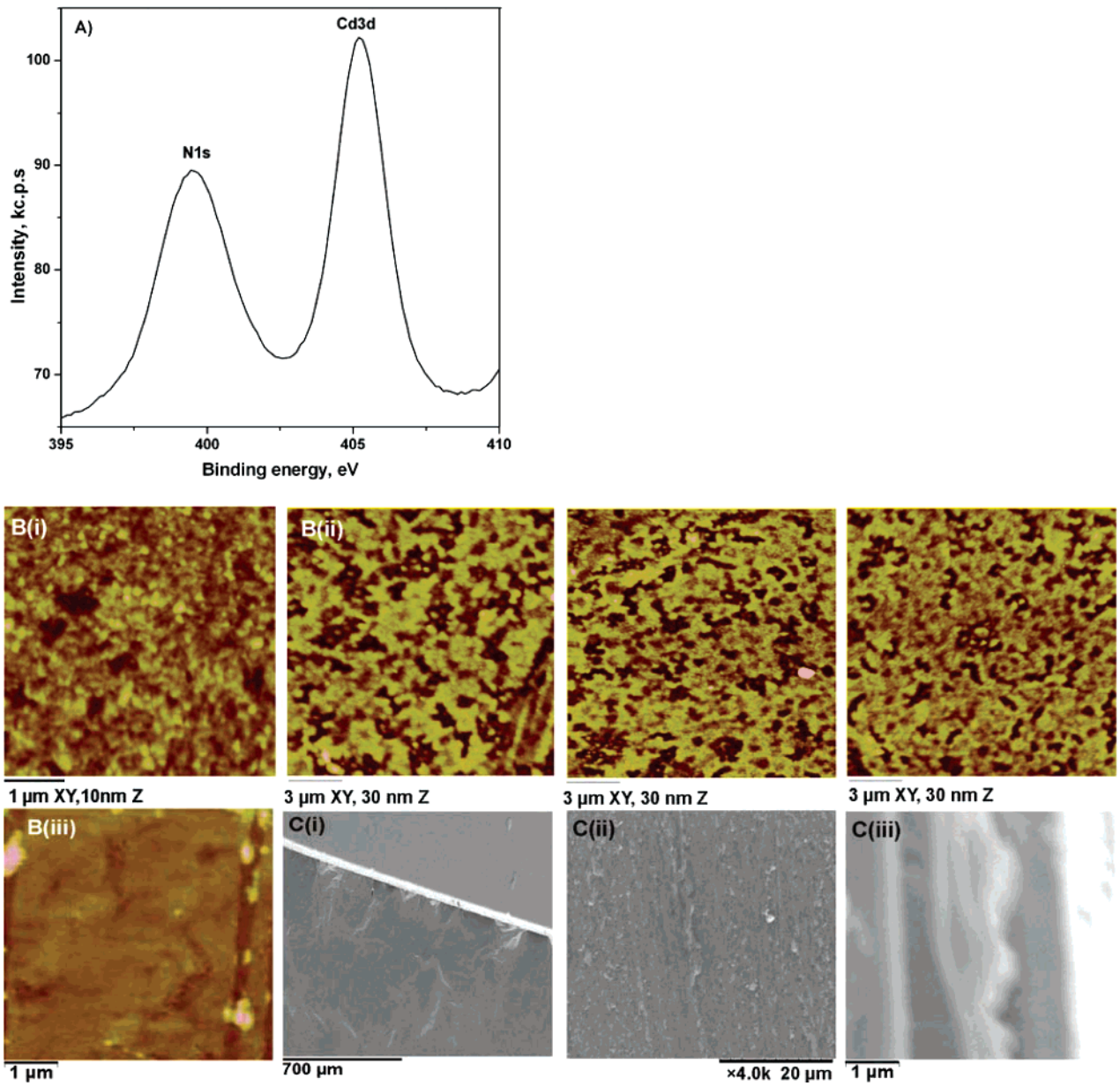

Figure 2. (A) XPS spectra of Cd^{2+} complexed 10-layer DTAR film using Mg Kα X-ray source (14 kV, 400 W). (B) AFM images in tapping mode, (i) 10-layer DTAR film with Cd^{2+}ions, (area, 1 μm *XY*, 10 nm *Z*), (ii) its surface morphology (area, 3 μm *XY*, 30 nm *Z*) at various cadmium concentrations (1.25, 0.75, and 0.25 μM), and (iii) aggregate structure of a polymer−probe composite observed using AFM. (C) SEM imaging, (i) at the membrane−glass interface (700 μm), (ii) DTAR film surface topography with Cd^{2+} on glass substrate (20 μm), with 4000 × order of magnification, and (iii) Cd^{2+} complexed DTAR monolayer pattern, a closer look.

to left). An AFM image of a polymer−probe L-B composite reveals a sheetlike aggregate structure, which might be caused by the certain degree of phase separation observed between the probe−polymer monolayers. SEM images recorded at the probe−substrate interface (marked as a thick line) reveal a smooth surface morphology, which showed some roughness with cadmium inclusion (Figure 2C).

Polymer Influence on Sensor Stability. For studies of the sensor stability, membrane strips of 22 probe layers were uniformly prepared under default conditions and their relative film stability was checked in terms of its absorbance intensity at λ_{max} 539 nm, after 45 min of equilibration at different pH conditions. Figure 3A depicts an unaltered film stability profile between pH 6.0 and 7.0. However, under extreme solution pH, desorption (leaching) of film monolayers was observed because of the fragile nature of the outer DTAR multilayers, held by a weak van der Waals force. The easy desorption of hydrophilic H_3L^+ and L^{2-} species, under acidic and alkaline conditions, was predicted as the major reason for such behavior. Consequently, for the intact position of the DTAR layers, a systematic study of the use of polymeric film coating for sensor protection was performed.

First, the nonspectral interference property of the PVOC polymer was checked by transferring PVOC3 film on a D22 (D denotes DTAR, and 22 indicates no. of monolayers) membrane strips. Changes in the absorption spectra were measured with and without PVOC. The peak intensity of the probe and its spectral properties were apparently unaltered in the presence of polymer monolayers, which showed similarity with PVS coatings. Study

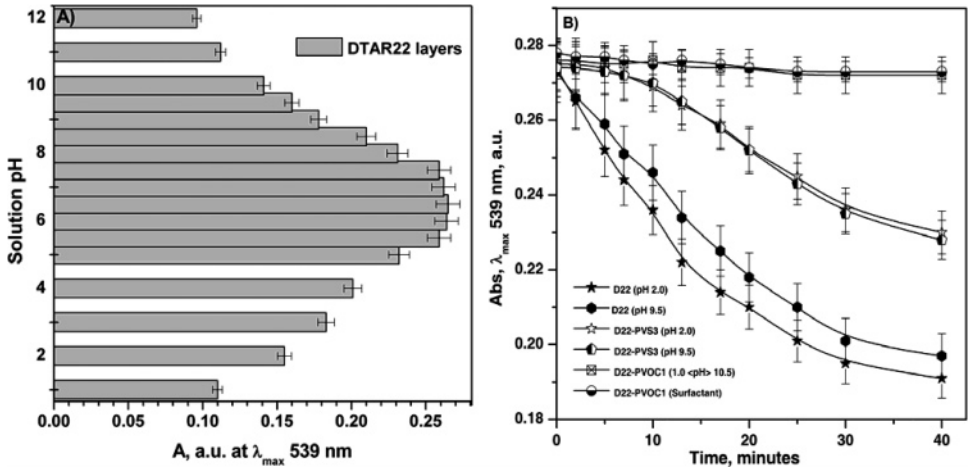

Figure 3. (A) Stability profile of D22 film sensors as a function of solution pH; (B) relative stability profile of D22 film sensors protected with polymer films, under extreme working conditions.

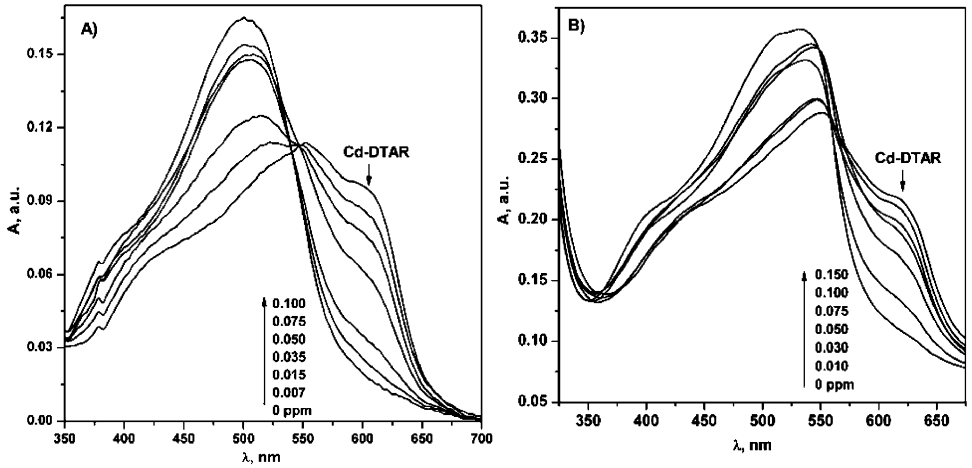

Figure 4. (A) Variation in absorption spectral profile for a D16−PVOC1 sensing system, with increasing cadmium concentration (mg/L) at pH 7.5 (10 min, 40 °C). (B) concentration-proportionate signal response for cadmium ions on D31−PVOC1 strips, batch equilibrated at pH 7.5 (20 min, 40 °C).

of the durability of a D22−PVOC3 film molecular assembly at extreme pH conditions of 2.0 and 9.5 revealed no great change in the signal intensity, thereby confirming the absence of probe leaching. Additional studies also confirmed that a single polymer layer (PVOC1) was sufficiently efficient for sensor protection. Because L-B films are prone to deteriorate in the presence of detergents and organics, a comprehensive study was performed on the sensor's stability in the presence of various surfactants (see Supporting Information). Interestingly, the polymer (PVOC) coating ensures a stable sensor assembly, even in the presence of major surfactants. However, similar studies performed with D22−PVS3 strips reveal a measurable probe loss attributable to the insufficient molecular interaction of the PVS monolayers ($\tau > 0.9$) with the DTAR membrane. Figure 3B represents the stability profile of a D22 L-B film sensor coated with a PVOC1 and PVS3 system, under rigorous experimental conditions. The surfactant presented in Figure 3B is 0.14 mM sodium lauryl sulfate, an anionic surfactant that is commonly used as an emulsifier in soaps and detergents.

Efficiency of Cadmium Sensing. The ion-sensing property of the sensor for cadmium ions as a function of solution pH (1−12) was tested with a series of D16−PVOC1 strips, using 5 μM cadmium solutions batch equilibrated for 45 min. The extent of cadmium chelation was studied before and after equilibration in terms of the relative changes in the sensor absorption spectra. Absorption spectra of the sensor assembly showed a bathochromic shift from 539 to 607 nm upon addition of Cd^{2+}, as a result of the formation of the charge-transfer complex. The relative absorbance at λ_{607} nm was at its maximum at pH 7.5 (MOPS buffer), with prominent color transition. However, an optimum pH range of 7.0−7.7 was selected for both quantitative and visual detection of cadmium (see Supporting Information). Because the ion-sensing property of the probe layers was prominent at near-neutral and slightly alkaline conditions, we recommend that the sample pH be adjusted within the optimum working range to achieve distinctive color transition and sensitive analysis for cadmium ions. Panels A and B in Figure 4 respectively show that the relative signal response for various cadmium concentrations as a function of probe monolayers was examined using D16−PVOC1 and D31−PVOC1 sensor strips.

The visual color transition profile observed on a D16−PVOC1 sensor system for various cadmium(II) concentrations (μg/mL) is shown in Figure 5A. The sensor strips exhibit a prominent color transition from its original yellowish orange to form a series of reddish-pink, pinkish-violet, and deep-purple complexes, with increasing cadmium content. The observed color change was

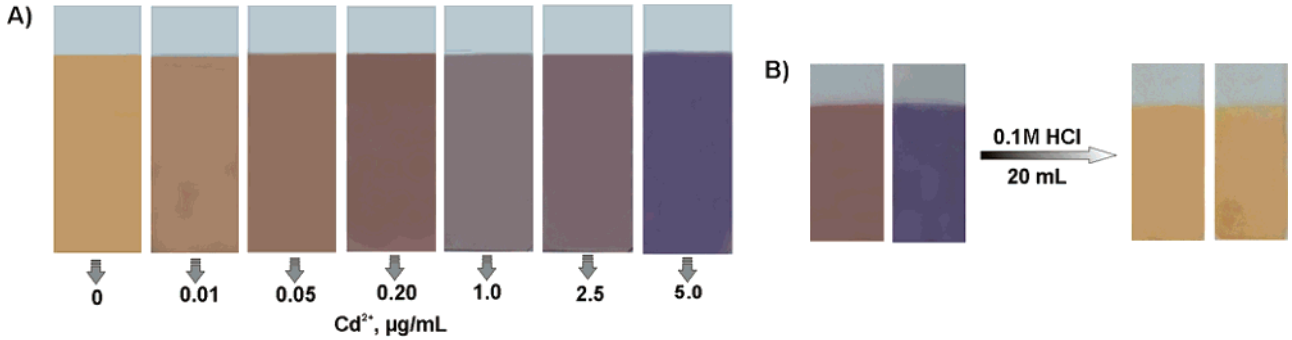

Figure 5. (A) Visible color transition pattern observed on a D16−PVOC1 multilayer sensor assembly mounted on the glass substrates, with increasing concentrations of cadmium ions (pH 7.5, 10 min, 40 °C). (B) A photographic image depicting the sensor instant regeneration from its cadmium complexes, with 0.1 M HCl.

stable even after 3 days' storage, with reproducible spectral data obtained on subsequent trials. Regeneration of the L-B film sensors was studied using both protolysis and a liquid-exchange reaction. In protolysis, a solution pH of <1 engendered spontaneous cadmium desorption from the sensor phase. However, to prolong the sensor life span, ligand exchange using 0.01 M EDTA was used for effective removal of cadmium ions after continuous equilibration for 40−45 min. The restored yellowish-orange strips were washed with water, and their absorption spectra were measured to elucidate the unaltered signal intensity at $\lambda_{max,}$ 539 nm. The sensor was reused for ion sensing up to 3−4 repeated cycles without loss of efficiency. The reversibility of the L-B film sensor strips, upon equilibration with a 20-mL volume of 0.1 mol/L hydrochloric acid, is depicted in Figure 5B.

Cadmium Response with Increasing Monolayers. With the intention of fabricating the most sensitive film sensor, six L-B film sensor assemblies, i.e., D62−PVOC1, D31−PVOC1, D24−PVOC1, D16−PVOC1, D10−PVOC1, and D6−PVOC1, were fabricated and their relative signal responses for cadmium ions were tested. With the D62−PVOC1 and D31−PVOC1 film sensors, the initial color contrast of the probe film was too intense to show the visual color transition for micromolar concentrations of cadmium ions. In addition, with increasing monolayers (>18), the sensitivity of cadmium detection <0.05 μM was prolonged to 40 min of equilibration at 30 °C. However, sensor assemblies ranging between D16−PVOC1 and D10−PVOC1 offer quantitative sensing of cadmium down to 0.05 μM, within 10 min of equilibration at 40 °C. The sensitivity and speed of reaction between cadmium and L-B film sensors increases considerably with decreasing DTAR monolayers. Using fewer monolayers enables faster and greater metal ion penetration through the probe molecular channels, which is not easily feasible with a dense membrane system, in spite of the sensor system exposure to high surface area. However, with the D6−PVOC1 system, because of the low chromophore content, it was difficult to perform naked-eye detection and an instrumental analysis was necessary for detection. Consequently, L-B film sensor strips of D10−PVOC1 and D16−PVOC1 assemblies were considered preferable for reliable visual and quantitative detection of cadmium ions at a rapid time scale.

The maximum response time required for cadmium signal saturation was monitored using a series of D16−PVOC1 and D31−PVOC1 glass strips, using 1 μM cadmium solution. Figure 6 shows that, to achieve prominent color transition and signal saturation at 20 °C, a time of 25−30 min was required for both

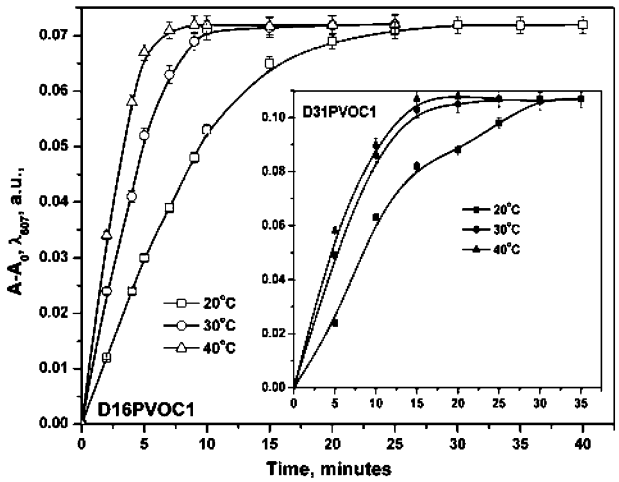

Figure 6. Temperature-dependent cadmium response kinetics for D16−PVOC1 sensor. The inset graph denotes the signal response for cadmium with D31−PVOC1 film sensor at pH 7.5.

D16−PVOC1 and D31−PVOC1 sensors. Experiments were performed at different temperatures (30, 40, and 50 °C) to elucidate the influence of the solution temperature on the rate of cadmium sensing. The time-proportionate signal response for cadmium ions at various solution temperatures was plotted against its relative absorbance at λ_{607} nm, with respect to the blank sensor (D31−PVOC1 and D16−PVOC1). It was interesting to observe that the response time was reduced to <10 and <20 min at 40 °C, for D16−PVOC1 and D31−PVOC1 systems, which could not be reduced further at even higher temperatures (>50 °C). It was inferred that the raised solution temperature enhances the kinetic energy of the aqueous-phase metal ions, thereby facilitating the faster diffusion-controlled exchange process through the dense probe membrane channels. The diffusion coefficient values (20 °C, 10 min) for cadmium ions were calculated to be 7.51×10^{-9} and 1.98×10^{-9} cm^2/s, with D16−PVOC1 and D31−PVOC1 strips, respectively, using the following expression, proposed by Zhang and Davison.[33]

$$D = M\Delta g/C_b tA \quad (1)$$

Therein, D is the diffusion coefficient of Cd^{2+} through the membrane of thickness Δg, at any time t and A is the exposed

(33) Zhang, H.; Davison, W. *Anal. Chem.* **1995**, *67*, 3391−3400.

Table 2. Tolerance Limits[a] for Various Inorganic and Complexing Species during Cadmium Sensing

cations	tolerance limit (mg/L)	anions	tolerance limit (mg/L)
Na^+/ K^+	8500/7525	Cl^-	8960
Ca^{2+}/Mg^{2+}	1750/1520	NO_3^-	7850
Ba^{2+}/Sr^{2+}	150/14.8	HCO_3^-	250
Fe^{3+}/Fe^{2+}	~12.5[b]	PO_4^{3-}	220
Co^{2+}/Ni^{2+}	4.55[b]/4.80[b]	F^-	350
Cu^{2+}/Zn^{2+}	4.75[b]/5.05[b]	Br^-	350
Mn^{2+}	2.35	NO_2^-	250
Bi^{3+}/Al^{3+}	10.6/11.5	SO_3^-	250
Cr^{6+}	12.0	SCN^-	70
As^{5+}	11.7	CO_3^{2-}	250
$Sn^{4+/2+}$	~11.2	citrate	220
Sb^{2+}	9.95	tartrate	255
Mo^{6+}	10.4	oxalate	250
Ti^{4+}	9.5	potassium biphthalate	340
La^{3+}	13.3	phthalate	340

surfactants	tolerance limit (mg/L)
cetyltrimethyl-ammonium chloride	78.0
tetraethylammonium -chloride	89.1
tetraamylammonium chloride	82.2
dilauryldimethyl-ammonium bromide	79.9
sodium dodecyl sulfate	44.5
Triton X-100	98.5
Triton N-101	100.2
humic acid	0.0011%

[a] Data denote quantities up to which no spectral interference was observed in cadmium (0.5 μM) sensing. [b] Maximum tolerance limit attained in the presence of masking agents during cadmium sensing.

membrane surface area. In addition, M is the mass of cadmium(II), which is defined as $M = C_m V_m$, where C_m is the cadmium ion concentration in the probe membrane of volume, V_m. Because the viscosity of the medium changes with temperature, the cadmium diffusion coefficients values at 30 and 40 °C were calculated using eq 2, where D_T is the diffusion coefficient at any

$$\log D_T = \frac{1.37023\ (T-20) + 8.36 \times 10^{-4}\ (T-20)^2}{109 + T} + \frac{\log D_{20}\ (273+T)}{293} \quad (2)$$

temperature T and D_{20} is the diffusion coefficient of Cd^{2+} at 20 °C, obtained from eq 1. The diffusion coefficient values were found to increase with temperature for both D16−PVOC1 and D31−PVOC1 sensors. For instance, the D_{30} and D_{40} values for cadmium(II) at 10 min with D16−PVOC1 sensor were calculated respectively as 3.69×10^{-8} and 1.04×10^{-7} cm^2/s.

Hybrid Probe−Polymer L-B Sensor. To enhance the performance of the L-B film sensor and to reduce the possible stages of time consumption without compromising the film quality, the combined use of polymer and chromophore was investigated. For this, appropriate ratios of DTAR and PVOC were prepared (90:10, 80:20, 60:40, 40:60, 20:80, 10:90) and transferred as hybrid multilayer composites in the form of 10−16 monolayers. The (π−A) isotherm plots for different ratios of DTAR/PVOC and DTAR/PVS were measured (see Supporting Information); their relative film stability and cadmium signal response were investigated. The stability of DTAR−PVOC mixed layers was studied in 2 M HCl solution, which revealed a mere ≤4% loss in the chromophore signal intensity, compared to a >60% loss for 100% DTAR (see Supporting Information). However, exposing the DTAR−PVS hybrid sensor assemblies to extreme acidities revealed probe leaching over time, underscoring the poor efficiency of the PVS layers.

Fabrication of hybrid L-B film composites was quick, but when subjected to time-dependent phase exchange, it exhibits a prolonged response time for cadmium sensing. Kinetic studies performed using a series of hybrid−sensor composites (DTAR/PVOC ratios of 85:15, 75:25, 70:30, 60:40, 50:50), to estimate the relative rate of cadmium (5 μM) signal response, confirmed this behavior. With lower DTAR ratios of 60:40 and 50:50, the elapsed time for signal saturation was longer (>20 min), which is apparently related to the net decline in the probe monolayers, aside from increasing PVOC content that might impair the free ion mobility through the probe molecular channels. In addition, the low color contrast associated with these hybrid assemblies hinders visual detection. However, at higher DTAR ratios (70:30, 75:25, 85:15), the cadmium visual sensing was good, with the sensing time limit slashed to <15 min for detection of 0.10 μM cadmium concentration at 40 °C. However, hybrid L-B composites of 90:10 or 95:5 (DTAR/PVOC) assemblies were unstable to sensing studies because of the inadequate polymer composition. It was also predicted that hybrid L-B composites (75:25−85:15) comprising more than 16 monolayers detected higher concentrations (≥μM) of cadmium, but were inappropriate for submicromolar cadmium concentrations.

Ion Selectivity and Matrix Tolerance Limits. The ion selectivity of the film sensor (D16−PVOC1) in detecting trace cadmium ions from multicomponent system was studied in terms of its matrix tolerance limits. For this study, 0.5 M each of K^+, Na^+, Cl^-, and NO_3^- and 0.01 M each of Ca^{2+}, Mg^{2+}, Ba^{2+}, F^-, Br^-, and SO_4^{2-} were used because they form a class of matrix components that are commonly found in major environmental samples. In addition, frequently encountered metal ions such as (10 μM) Mn^{2+}, Fe^{2+}, Fe^{3+}, Co^{2+}, Ni^{2+}, Cu^{2+}, Zn^{2+}, Bi^{3+}, and Al^{3+} and anions such as (2.5 mM) HCO_3^- and PO_4^{3-}, which might coexist with cadmium ions in wastewater samples, were also investigated. However, Table 2 shows that the tolerance limits for the studied foreign ions were established individually by batch equilibration with 0.5 μM cadmium solutions, to the maximum limit to which cadmium ions were found to be spectrally free from interference. The analytical data reveal that most of the matrix species showed no significant interference, except Ba^{2+}, Fe^{3+}, and SO_4^{2-} ions, which slightly prolonged the reaction time. Interference from ferric ions was eliminated using 0.2 mM pyrophosphate solution prior to analysis. Apart from this, Cu^{2+}, Co^{2+}, Ni^{2+}, and Zn^{2+} ions were found to exhibit positive interference when greater than 0.61 ppm. However, these ions were eliminated quantitatively up to ≤5.0 ppm by adding a mixture 0.25 mM thiosulfate, citrate,

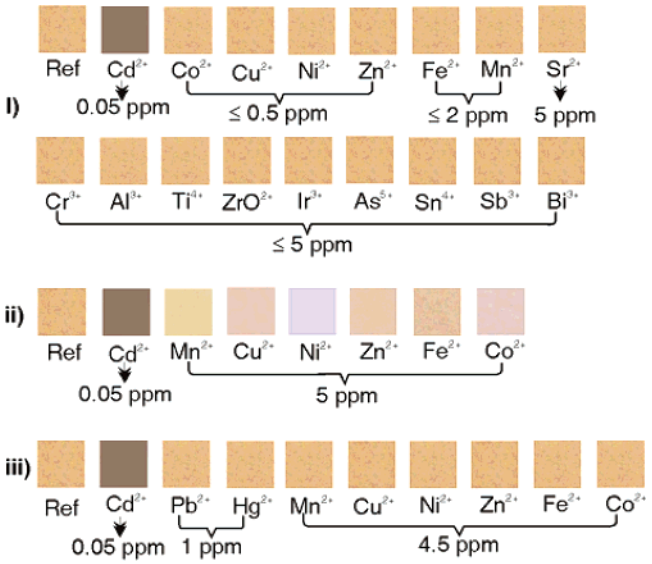

Figure 7. (i) Ion-selectivity photographic profile depicting the degree of tolerance achieved for various matrix constituents on a D16−PVOC1 L-B film sensor, (ii) relative color transition observed for interfering metal ions present in 100-fold excess over cadmium ions, and (iii) cadmium selectivity with respect to other toxic ions (20−90-fold excess), which were suppressed beyond their tolerance limit.

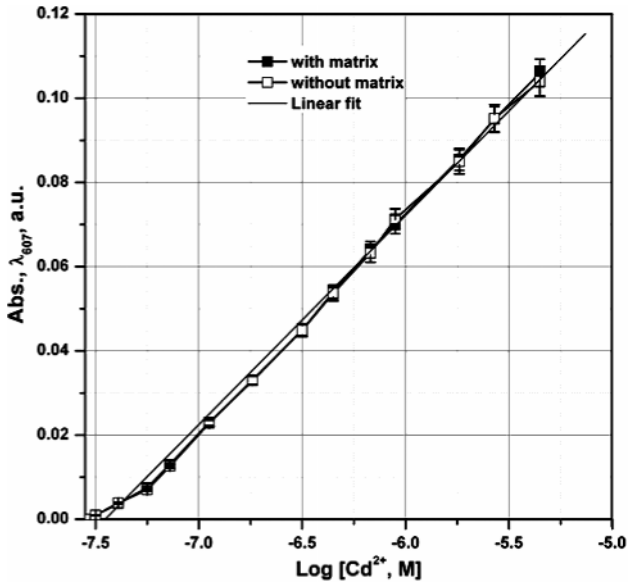

Figure 8. Normalized linear calibration plot for a cadmium-complexed D16−PVOC1 film assembly. Data points denote the absorbance difference at λ 607 nm, with respect to a blank D16−PVOC1 sensor.

and tartrate solution along with MOPS buffer. Tolerance studies were also extended to some toxic heavy metal ions, $Sn^{2+/4+}$, Sb^{2+}, As^{5+}, As^{3+}, Mo^{6+}, Cr^{6+}, Bi^{3+}, and Al^{3+}, which were found non-competent for the chelating sites and hence did not cause any serious interference. However, beyond their tolerance limits (listed in Table 2) they showed negative interference resulting from the increasing ionic strength of the medium. However, Pb^{2+} and Hg^{2+} ions were found to be partly competitive under these conditions; they were suppressed using 0.15 mM oxalate and citrate, up to 1.5 ppm. The sensor's visual transition for cadmium (0.05 ppm) is highlighted in Figure 7 in comparison with various foreign ions. Because surfactants (cationic, anionic, and nonionic) are known to play an influential role in both L-B film durability and the ion-sensing process, prominent surfactants that are commonly used were examined. Interestingly, aside from sodium dodecyl sulfate, which, when greater than 45 mg/L concentration, was found to enhance the probe initial optical intensity, the surfactants were ineffectual, even beyond 75 mg/L, which is an added advantage of using these sensor strips.

Calibration Graph and Statistical Analysis. The concentration-proportionate absorption spectra for cadmium were measured, and their relative absorbance was normalized with respect to blank sensors at λ_{607} nm. A linear calibration graph in the cadmium concentration range of 0.025−4.46 μM was achieved, with a coefficient of determination (r^2) of 0.996 (Figure 8). The detection (L_D) and quantification (L_Q) limits were determined from the plot using eqs 3 and 4,[34] which were estimated respectively as 0.039 and 0.050 μM. To validate the precision and accuracy of the method, seven successive measurements were performed for 0.31 μM cadmium using D16−PVOC1 sensor strips at pH 7.5 (40 °C, 10 min). The relative standard deviation for the analysis was calculated as 0.259%.

$$L_D = k_1 S_b / m \quad (3)$$

$$L_Q = k_2 S_b / m \quad (4)$$

Therein, S_b represents the standard deviation of the signal response for the blank, m is the slope of the linear calibration range, $k_1 = 3$, and $k_2 = 10$.

APPLICATION

Sensing Cadmium from a Synthetic Mixture. The practical utility of the sensor strip in detecting ultratrace cadmium ions from a wastewater sample was tested using a simulated synthetic solution containing 5500 mg/L Na^+ and K^+, 750 mg/L Ca^{2+} and Mg^{2+}, 2.0 mg/L Mn^{2+}, Cu^{2+}, Ni^{2+}, and Co^{2+}, and 10 mg/L Fe^{2+} and Zn^{2+} ions, along with 6000 mg/L Cl^- and NO_3^- and 400 mg/L SO_4^{2-}, F^-, and Br^- ions. To this composite, 0.010 mg/L cadmium ions was spiked and equilibrated under optimum conditions. The corresponding spectral changes of D16−PVOC1 strip were monitored, and the normalized absorbance at 607 nm was fitted into the calibration plot, which showed a value of 9.88 ± 0.5 μg/L (95% CL), for triplicate measurement (RSD 3.1%).

Targeting Cadmium from Spiked Real Samples. Quantitative estimation of submicromolar levels of cadmium was attempted from various real sample effluents collected from different sources including a food processing factory, a semiconductor fabrication facility, quartz manufacturing facility, and a local hospital. Because the real samples subjected to the current analysis were pretreated, cadmium-sensing amid the multicomponent system was viewed using an internal standard addition method. The samples were filtered and first subjected to ICP-AES analysis to measure the possibility of detecting any toxic metal ions, but only 15.7−265

(34) Christian, G. D. *Analytical Chemistry,* 6th ed.; John Wiley & Sons Inc.: New York, 2003; pp 112−113. Skoog, D. A.; Holler, F. J.; Nieman, T. A. *Principles of Instrumental Analysis*, 5th ed.; Thomas Asia Pty. Ltd.: Singapore, 2005; pp 13−14.

Table 3. Determination of Spiked Cadmium Ions from Industrial and Domestic Effluents

		Cd^{2+} (μg/L)	
effluent source	spiked amount	amount added	amount found
food processing factory	10 mg/L Ca^{2+}, Mg^{2+}; 1.0 mg/L Co^{2+}, Cu^{2+}, Ni^{2+}, Zn^{2+}, Fe^{2+}; 0.05 mg/L Mn^{2+}; 0.2 mg/L Sn^{2+}, Sb^{2+}; 250 mg/L Na^{+}, K^{+}	10 20	10.90[b] (3.8) 20.29[b] (2.7)
quartz manufacturing facility	0.5 mg/L Si^{4+}; 0.15 mg/L Bi^{3+}, Tl^{+}, Ga^{3+}, Ir^{3+}; 0.10 mg/L La^{3+}, Ce^{4+}, Nd^{3+}, Sm^{3+}	10 20	11.24 (3.6) 19.90 (2.8)
semiconductor fab	0.25 mg/L Bi^{3+}, Al^{3+}, Tl^{+}, Ga^{3+}, Ir^{3+}; 0.10 mg/L La^{3+}, Ce^{4+}, Nd^{3+}, Sm^{3+}; 0.5 mg/mL Ni^{2+}, Co^{2+}, Mn^{2+}; 10 mg/L Ca^{2+}, Mg^{2+}; 0.5 mg/L − Si^{4+}	15 20 35	13.38[b] (4.3) 18.73[b] (3.8) 36.32[b] (3.8)
local hospital effluent	1.75 mg/L Cu^{2+}, Ni^{2+}, Zn^{2+}, Mn^{2+}, Fe^{2+}; 15 mg/L Ca^{2+}, Mg^{2+}; 275 mg/L Na^{+}, K^{+}	6.5 15	5.93[b] (4.1) 14.16[b] (4.0)

[a] Values in parentheses denote relative standard deviations for triplicate measurements. [b] Data obtained after eliminating foreign ions was beyond their noninterference limit.

mg/L alkali and alkaline earth metal ions were detected, aside from traces (0.02−0.083 mg/L) of Zn^{2+}, Mn^{2+}, and Fe^{2+} ions. The studied samples were used as a precursor to test the sensor's practical implementation in real samples. Consequently, Table 3 shows that a known amount of foreign ions that might coexist in the effluent solution was added to the effluent samples, along with a trace amount of cadmium ions. The spiked effluent solutions were batch-equilibrated with D16−PVOC1 membrane strips and fabricated under default conditions. Then, the sensing was performed at 30 °C, under optimum experimental conditions. The analytical data indicate the promising aspect of the fabricated L-B film sensor as a potential candidate for monitoring environmental and synthetic samples. It is also noteworthy that the levels of foreign ions spiked to these samples were many times greater than any industrial or domestic effluent samples that one might reasonably encounter in the present day, based on the regulatory laws of waste disposal and environmental pollution.

SUMMARY

In this work, visual and quantitative sensing of trace cadmium ions was undertaken using nanoassemblies of amphiphilic chromoionophore molecules anchored on microscopic glass slides and covered with polymer monolayers. This demonstration of chromoionophore monolayers as a naked-eye sensing tool for cadmium ions presents the first example of a new class of solid-state colorimetric ion sensors using L-B thin-film methodology. The present film sensor offers good ion selectivity for cadmium that is useful for sensitive detection of low microgram per liter levels of cadmium ions from synthetic and environmental samples. Interestingly, the film sensor exhibits greater durability and complete reversibility, which markedly reduces costs for these types of sensor. The salient features, such as naked-eye sensing, faster exchange kinetics, portability, and storability, render the present solid sensor a perfect testing kit for on-site field analyses.

ACKNOWLEDGMENT

This work was financially supported by the Japan Society for the Promotion of Science (JSPS).

SUPPORTING INFORMATION AVAILABLE

Synthesis (Scheme S1) and spectral characterization of probe, 4-*n*-dodecyl-6-(2-thiazolylazo)-resorcinol). Characterization of probe molecular assemblies (D**2**) by ATR-FT-IR spectra (Figure S1). Influence of sample pH on cadmium signal response (Figure S2). Isotherm plot for probe−polymer hybrid sensor (Figure S3) and its relative stability (Figure S4). Influence of surfactants on sensor stability (Figure S5). This material is available free of charge via the Internet at http://pubs.acs.org.

Received for review December 13, 2006. Accepted March 23, 2007.

AC0623540